Proceedings of the ASME Turbo Expo 2013
GT2013
June 3-7, 2013, San Antonio, Texas, USA

GT2013-95662

EXPERIMENTAL AND NUMERICAL STUDY OF PARTICLE INGESTION IN AIRCRAFT ENGINE

Maria Grazia De Giorgi* †
University of Salento
Dep. Engineering for Innovation
Lecce, Italy
mariagrazia.degiorgi@unisalento.it

Stefano Campilongo
University of Salento
Dep. Engineering for Innovation
Lecce, Italy
stefano.campilongo@unisalento.it

Antonio Ficarella†
University of Salento
Dep. Engineering for Innovation
Lecce, Italy
antonio.ficarella@unisalento.it

Mauro Coltelli
Istituto Nazionale di Geofisica e Vulcanologia
Osservatorio Etneo - sezione di Catania (Italy)
mauro.coltelli@ct.ingv.it

Valerio Pfister
ENEA
Technical Unit for Material Technologies
Brindisi, Italy
valerio.pfister@enea.it

Francesco Sepe
ENAC
Italian Civil Aviation Authority
Roma, Italy
f.sepe@enac.gov.it

ABSTRACT

This study is focused on volcanic ash ingestion in aircraft engines, that can lead to slow but constant deterioration in engine performance and engine failure because of the mechanical damages to the wall surface. In particular the particles that impact on blades surfaces cause erosion damage and permanent losses in engine performance. Aircraft engine fans could be severely damaged by the ash flow.. In order to clarify the erosion phenomenon the fan has been simulated through the general-purpose CFD code and the numerical simulations were performed using the Reynolds–Averaged Navier–Stokes (RANS). After validating the numerical modeling of the flow without erosion by comparisons with experimental data in literature, a surface injection of a discrete phase has been introduced in order to evaluate particle ingestion of volcanic ash. This phenomenon is a typical gas-particle two-phase turbulent flow and a multi-physics problem where the flow field, particle trajectory and wall deformation interact with among others. A wide experimental investigation has been carried out on an ash sample from Etna volcano. In particular a sieve analysis to obtain particles dimensional distribution and an analysis of SEM images to calculate particles shape factor. These data were used to modeling the particle injection in the CFD model. The numerical investigation was aimed to clarify the effects of particle erosion and to evaluate the change of the flow field in the case of eroded blades. By erosion rate patterns, the eroded mass was estimated and it was used to model the eroded geometry, by a user routine implemented in the dynamic mesh module of the code. So the performances of the damaged fan were estimated and compared with the baseline geometry without erosion.

INTRODUCTION

Volcanic eruptions can eject large amount of solid and gaseous material into the atmosphere. Large, solid particles precipitate from the atmosphere close to the volcano but small particles and gaseous material can be moved to high altitudes and dispersed far away by atmospheric phenomena. The smallest particles which are less than 0,1 mm can stay in the atmosphere for two or three years after a volcanic eruption These ash particles typically have a melting point of approximately 1000°C. Sulfur compounds and other aerosols can be in ash clouds. At high altitudes, ice may form on ash particles, and electrostatic charges may also be present on ash particles. In recent past years several commercial aircrafts have unexpectedly experienced volcanic ash in flight and at airports [1]. Part of these encounters caused varying degrees of in-flight loss of jet engine power [2]. The damage on aircraft that fly through an eruption cloud depends on the concentration of volcanic ash and gas aerosols in the cloud, the length of time the aircraft actually spends in the cloud, and the actions taken by the pilots to exit the cloud [3].

∗Address all correspondence to this author.
†ASME Member.

Ash ingested by jet engines can lead to an immediate deterioration in engine performance and cause engine flameout. Ash can also damage moving engine parts, as compressor and turbine blades, reducing engine efficiency. Molten ash can solidify inside cooling passages, blocking the passages and reducing cooling airflow, increasing blade temperatures, and reducing engine life.

Volcanic ash is highly abrasive. It consists of hard, sharp rock fragments that could erode plastic, glass, and metals.

Aircraft engines operating in presence of volcanic ash are subjected to the performance and lifetime deterioration due to particle erosion, in particular on fan and compressor blades

The erosion of fan and compressor blades causes an increase of blade surface roughness and tip clearances, a change of the blade leading edge characteristics and a reduction of the blade chord with a subsequent degradation in performance [4,5].

In literature several performance deterioration models have been developed for compressors in order to predict the effects of erosion [6], and fouling [7] on the stage pressure, work and efficiency.

Erosion in turbomachinery is influenced by many factors such as the ingested particle characteristics, gas flowpath, blade geometry, operating conditions, and blade material [8]. Grant and Tabakoff [9] and Balan and Tabakoff [10] conducted experimental studies on single-stage axial-flow compressor erosion. Examination of disassembled rotor blades after sand ingestion revealed blunted leading edges, sharpened trailing edges, reduced blade chords, and increased pressure surface roughness. Rotor-blade erosion was evident in particular in the outer 50% of the span, where significant reductions in the blade chord and thickness and changes in the leading- and trailing-edge geometries were observed

In recent years, erosion phenomenon has been numerically investigated. In several previous works, however, the change of the flow field and the relating particle trajectory over the eroded geometry were not taken into account.

In [11] the “erosion line” approach has been adopted, in order to reproduce a sand erosion phenomenon; in this approach, an erosion cavity is approximated by a line, taking into account the hypothesis that the width of erosion cavity is sufficiently small, compared with the three-dimensional grid spacing on a wall surface. Another way can be found in [12], where a parametric CAD model of eroded blades is presented with a probabilistic approach for performance analysis.

The prediction of erosion in turbomachinery is complex due to the tracking of particles through the flow field in addition to different parameters as rotational speed, operating conditions, blade geometry and material, particle dimensions, rebound and fragmentation.

Numerical investigations of particle trajectory are based on Eulerian–Lagrangian approach with one-way coupling between particles and flow, in association with erosion correlations.

In literature several prediction correlations were implemented, as in [13] where the rate of erosion was given in terms of particle mass and impact velocity.

Other erosion models were developed in [14-16]. A comparison between different erosion models is given by Dobrowolsky and Wydrych [17].

In last years many researchers developed different numerical models to predict erosion rate on turbomachinery components. Corsini et al. [18] performed a numerical study to clarify the influence of fan aerodynamic operation to the determination of erosion regimes and patterns. In [19] a numerical study of particle dynamics and erosion in a high pressure axial turbine stage was presented. On the pressure side, regions of dense erosion were observed in proximity of the leading edge and trailing edge as well as the tip corner.

In [20] blade surface erosion was predicted by numerical blade surface statistical impact data from particle trajectory simulations with correlations of erosion test results for blade and coating materials.

Erosion rate is affected by particle composition and shape. Particle shape is highly variable on the basis of products of different eruptions or different size classes of the same deposit [21] and it is important for the definition of the drag parameters; in [22] the authors developed a complete characterization of the ash particles erupted on December 2002 from Etna volcano in Italy to evaluate the terminal velocity. In the present work we used a sample of ash from Etna volcano for our in-house dimensional and morphological characterization. Surface area of volcanic ash particles is of great importance to research including plume dynamics, particle chemical and water reactions in the plume [23].

In the present work the transonic axial fan NASA Rotor 67 was used as test case. In literature several experimental [24] and computed [25-27] data are available for this geometry. First the numerical simulations have been performed for the baseline configuration of the rotor; then an injection of particles has been introduced in the model, after an experimental characterization of an ash sample. Finally the eroded mass was estimated by calculated erosion rate patterns and it was used to model the eroded geometry, by a user routine implemented in the dynamic mesh module of the CFD code. So the performances of the damaged fan were estimated and compared with the results of baseline geometry.

CHARACTERIZATION OF VOLCANIC ASH SAMPLE

The characterization of the volcanic ash particles is necessary for a better prediction of the erosion phenomena on fan. So a sample of volcanic ash from Etna volcano provided by Italian National Institute of Geophysics and Volcanology was characterized (fig. 1). The aim of this analysis was also the implementation of a methodological approach to characterizing ash sample, in terms of dimensional and morphological particles data. The analyzed sample weights 133,56 g for a volume of 93 cm^3.

Particle dimensional analysis

Particles size is an important factor to assess the effects of their impact on blades surface. In this study standard sieve (ASTM 1181) has been used to evaluate the size distribution, reported in fig. 2; more than 70% of the sample has a dimension bigger than 63 µm. A Rosin-Rammler distribution has been used to implement this particle distribution in the CFD code. The full range of sizes is divided into an adequate number of discrete intervals, each represented by a mean diameter for which trajectory calculations are performed. The mass fraction of particles with a diameter greater than *d* is given by:

$$Y_d = e^{-(d/\bar{d})^n} \quad (1)$$

where particle diameter $\bar{d}$ is a mean diameter and n is the so-called spread parameter; in our case we set 82 µm and 3.36 respectively.

Figure 3 depicts the Rosin-Rammler distribution compared with experimental data. Minimum and maximum diameters are 7 and 180µ m respectively .

Morphological characterization

Discrete phase trajectory is strongly influenced by particles shape. The drag coefficients for spherical particles were initially obtained experimentally with particle diameter, d_p, as the characteristic length. Usually, studies on non-spherical particles use the volume equivalent spherical diameter as the characteristic length. Therefore shape description is a significant issue in two phase flow studies. Various shape factors have been defined and used to describe shape effect of non-spherical particles, regular or irregular, including particle sphericity, particle circularity, Corey shape factor and Stokes shape factor, summarized in [28].

This work's step is focused on the acquisition and post-processing of two-dimensional digital images carried out by scanning electron microscopy (SEM) to obtain shape parameters by image analysis. Microstructural observations were performed by ENEA Technical Unit for Brindisi Material Technologies. Figure 4 shows a typical SEM image.

Then a tool was developed by authors in LabView [29] able to read an image, to identify particle in a defined dimensional range (red bounding lines in fig. 4), and to calculate several particle shape factors, such as aspect ratio, center of mass, area, etc.

For the purpose of the present study, we were interested to the sphericity defined as the ratio of the surface area of a sphere (with the same volume as the given particle) to the surface area of the particle:

$$\phi = \frac{A_{sph\_V}}{A_P} \quad (2)$$

By this analysis a mean sphericity value equal to 0,68 was found.

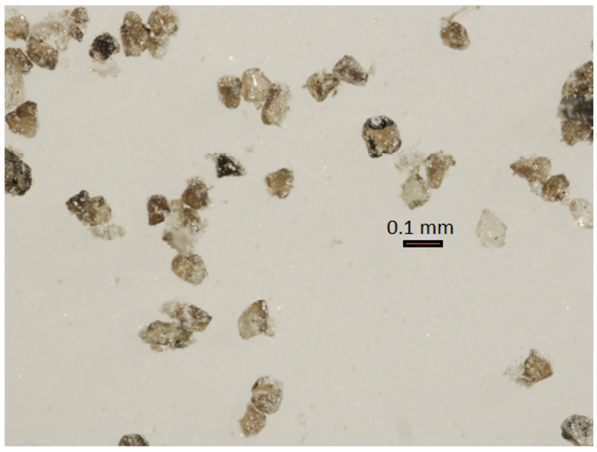

Figure 1. VOLCANIC ASH SAMPLE.

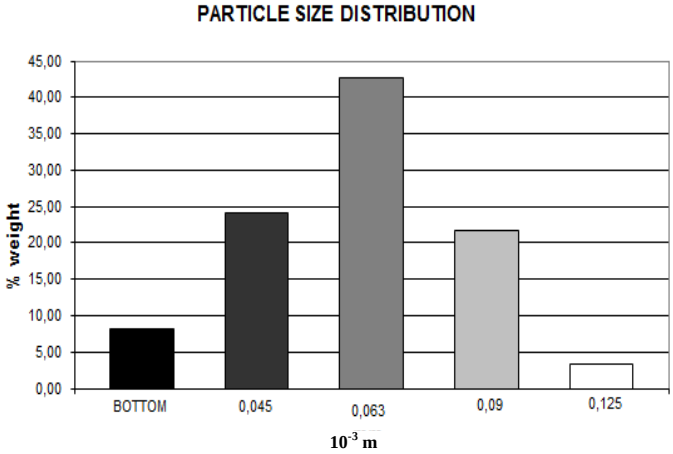

Figure 2. SAMPLE SIZE DISTRIBUTION.

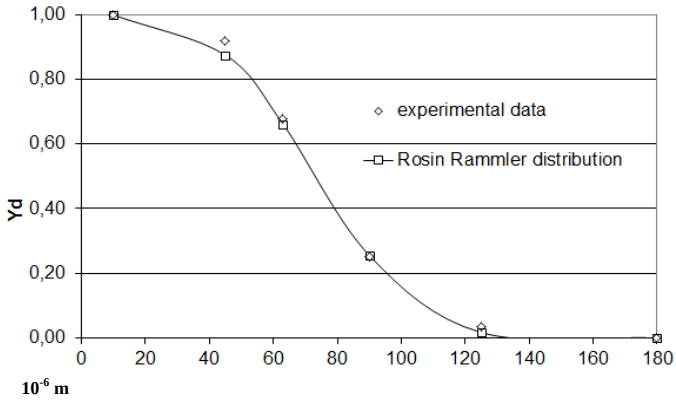

Figure 3. COMPARISON BETWEEN ROSIN-RAMMLER DISTRIBUTION AND EXPERIMENTAL DATA.

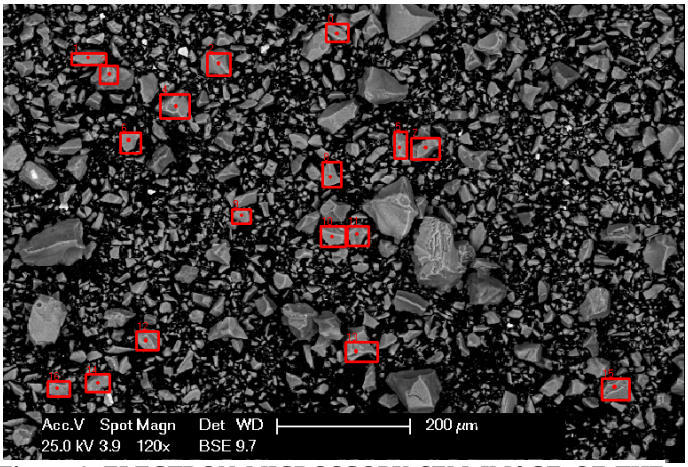

Figure 4. ELECTRON MICROSCOPY SEM IMAGE OF THE SAMPLE.

NUMERICAL APPROACH

The CFD code ANSYS Fluent 14 [30] was used to calculate the flow field around the rotor. The code employs the finite volume method with second order upwind scheme for discretizing the convection terms in the momentum transport equations. The gas-phase is assumed to be a continuum phase, while the particle volcanic ash is a dispersed phase. The gas-phase flow is considered compressible and turbulent.

In the present work the k-ε Realizable turbulence model of Shih [36], with second order accuracy, was used. This model has been extensively validated for a wide range of flows [36, 37], also in turbomachinery, in the case of boundary layer flows under strong adverse pressure gradients or separation, rotation, recirculation and strong streamline curvature. For all these cases, the performance the model has been found to be substantially better than that of the standard k- ε model.

The computational procedure for the prediction of the performance of the eroded blades was as follows:

- Calculate the turbulent flow field of the baseline configuration.
- Insert particles injection and calculate the particle trajectories.
- Evaluate erosion rate patterns and estimate the amount of erosion.
- Modeling of the eroded blades wall shape by using a dynamic mesh approach.
- Numerical simulation of the flow field to estimate the performances of the fan with eroded blades.

Particle motion theory

The CFD code predicts the trajectory of a discrete phase particle by integrating the force balance on the particle, which is written in a Lagrangian reference frame. This force balance takes into account the particle inertia with the forces acting on the particle, and can be written [31] as:

$$\frac{dV_P}{dt} = F_D(V - V_p) + \frac{g(\rho_P - \rho)}{\rho_P} + F \tag{3}$$

Where F is an additional acceleration (force/unit particle mass) term, $F_D(V\text{-}V_p)$ is the drag force per unit particle mass with the coefficient F_D equal to:

$$F_D = \frac{18\mu}{\rho_P d_P^2}\frac{C_D \,\mathrm{Re}}{24} \tag{4}$$

$$\left|V - V_p\right| = \sqrt{(u-u_p)^2 + (v-v_p)^2 + (w-w_p)^2} \tag{5}$$

Here, V is the fluid phase velocity, V_p is the particle velocity, u,v,w are longitudinal, lateral and vertical velocity respectively; ρ is the fluid density, ρ_p is the density of the particle, and d_p is the particle diameter. *Re* is the relative Reynolds number, which is defined as

$$\mathrm{Re} = \frac{\rho d_P \left|V_P - V\right|}{\mu} \tag{6}$$

Equation (3) incorporates additional forces in the particle force balance that can be important under special circumstances.

In eq. (4) C_D is the aerodynamic drag coefficient, dependent on the Reynolds number in eq. (6). There are many studies of drag coefficients for fixedly, regularly shaped particles reported in the literature [31, 32]. These drag models are accurate only for the selected shapes and orientations. We chose the correlation proposed by Haider and Levenspiel [33] for spherical and non-spherical particles based on more than 500 experimental data points:

$$\mathrm{C_D} = \frac{24}{\mathrm{Re_{sph}}}(1 + \mathrm{b_1 Re_{sph}^{b_2}}) + \frac{b_3\,\mathrm{Re}_{sph}}{b_4 + \mathrm{Re}_{sph}} \tag{7}$$

With:

$$b_1 = \exp(2{,}3288 - 6{,}4581\phi + 2{,}4486\phi^2) \tag{8a}$$

$$b_2 = 0{,}0964 + 0{,}5565\phi \tag{8b}$$

$$b_3 = \exp(4{,}905 - 13{,}8944\phi + 18{,}4222\phi^2 - 10{,}2599\phi^3) \tag{8c}$$

$$b_4 = \exp(1{,}4681 + 12{,}2584\phi - 20{,}7322\phi^2 + 15{,}8855\phi^3) \tag{8d}$$

In the last equation ϕ is the particle parameter as defined in eq.(2).

Particle-Tracking theory

For the dispersion of particles due to turbulence in the fluid phase the stochastic tracking model was used. This random walk model includes the effect of instantaneous turbulent velocity fluctuations on the particle trajectories through the use of stochastic methods. Instead the other approach for the

computation of particle trajectory is the cloud model [34], which tracks the statistical evolution of a cloud of particles about a mean trajectory. The concentration of particles within the cloud is represented by a Gaussian probability density function.
The instantaneous value of the fluctuating gas flow velocity, is given by:

$$u = \bar{u} + u' \tag{9}$$

It is the sum of mean and instantaneous velocity; it is used to predict the dispersion of the particles due to turbulence.
Particle trajectory is calculated by integrating the equation (3) for individual particles along the particle path during the integration. By computing the trajectory in this manner for a sufficient number of representative particles (termed the "number of tries"), the random effects of turbulence on the particle dispersion may be accounted for. The fluctuating velocity components have a random value kept constant over an interval of time given by the characteristic lifetime of the eddies.
Prediction of particle dispersion makes use of the concept of the integral time scale, T , which describes the time spent in turbulent motion along the particle path, *ds*:

$$\mathrm{T} = \int_0^{\infty} \frac{u_p'(t)u_p'(t+s)}{\overline{u_p'^2}} ds \tag{10}$$

The integral time is proportional to the particle dispersion rate.

Erosion model

The flow prediction is used to derive the drag forces imparted by the fluid on the particles; hence the trajectories of a large number of particles are predicted. When individual particles impact on a wall the damage is evaluated by empirical impact damage relationships. The average impact damage of a large number of particles can then be used to predict the distribution and depth of erosion damage on a surface. There are many known methods of erosion rate calculations, in the present work the erosion rate ER is a modified form of equation of Huser & Kvernvold [35], it is calculated as:

$$ER = \sum_{P=1}^{Nparticles} \frac{\dot{m}_p \, C(d_p) f(\alpha) v^n}{A_{face}} \tag{11}$$

expressed in kg/ (m^2s) as unit, where $C\ (d_p)$ is a function of particle diameter, α is the impact angle of the particle path with the wall face, $f\ (\alpha)$ is a function of impact angle, v is the relative particle velocity, n is a function of relative particle velocity, and A_{face} is the area of the cell face at the wall.
The adopted values are: $C=1.8*10^{-9}$, n = 2.6 as in [35], with an impact angle calculated by the software for each different node.

Computational model and test case

In this work the test case is the NASA Rotor 67 fan, a transonic axial fan rotor with low aspect ratio designed by NASA in 1970s (in table 1 nominal data are listed). Laser measurement data for this rotor has been reported by Strazisar [24]. The computational domain is generated by the software GAMBIT. The computational grid of hub and blade walls (pressure, suction and tip) is shown in fig. 5 and fig. 6. The total number of cells is about 800000. The mesh quality is characterized by a skewness value of 97%. The dimensionless wall distance, y+, at the wall boundaries was fixed to a value close to 5.
The inlet and outlet boundaries are located at station 1 and station 2, used in [24]. Experimental profiles of total temperature, total pressure and flow angle at inlet and static pressure at the outlet are used as boundary conditions.
Periodic flow conditions are imposed on the lateral faces of the flow domain.
The materials of solid particles and walls were assumed to be quartz and steel, respectively. In the modeling of volcanic particle injection, the particle distribution has been set as reported previously in the section “Particle dimensional analysis”. The particle concentration was set equal to 1000 mg/m^3 equally distributed across the fan. In the particle trajectory calculation, the rebound velocity at the blade surface is estimated by using erosion model. In the rebound at end walls, particle impingement is treated as perfect elastic impingement.

Table 1. NASA ROTOR 67 CHARACTERISTICS

Number of blades	**22**
Design pressure ratio [-]	**1.63**
Rotational speed [rpm]	**16043**
Diameter [cm]	**51.4**
Aspect ratio	**1.56**
Design mass flow rate [kg/s]	**33.25**
Tip leading edge speed [m/s]	**429**

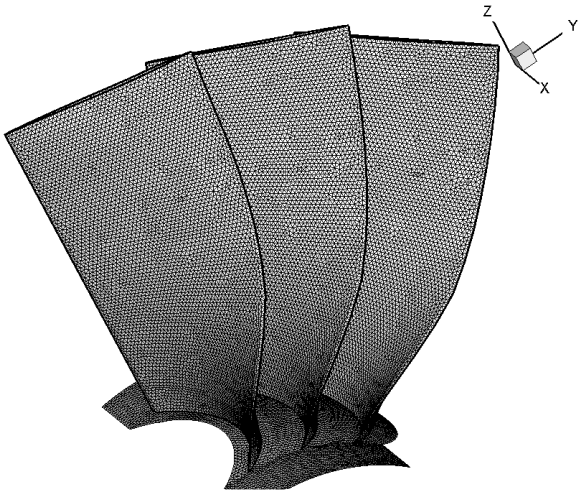

Figure 5. ROTOR 67 GRID OF THE HUB AND BLADE WALLS.

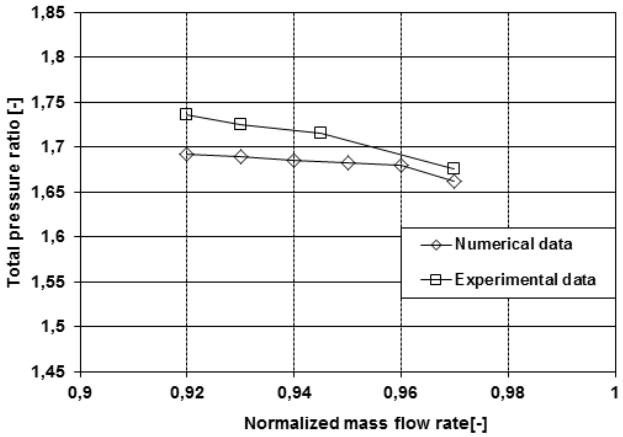

Figure 6. PRESSURE RATIO, COMPARISON BETWEEN NUMERICAL AND EXPERIMENTAL DATA [24].

RESULTS

Validation case without particle injection

The validation has been done at different mass flow rates modeling the flow without particle injection. The design rotational speed is 16043 rpm, and the tip leading edge speed is 429 m/sec with a tip relative Mach number 1.38. The predicted total pressure ratio at full speed are plotted versus normalized mass flow and compared to experimental data. The computational results are in agreement with the experimental data. Figure 6 shows a comparison between experimental and numerical pressure ratio data, and then the predicted total pressure contour is shown in fig. 7.

Figure 8 shows the steady-state relative Mach number contours at 30% spanwise distance from the hub, for the design mass flow rate. The experimental data are shown on the left, the computational results on the right. The results indicate that the

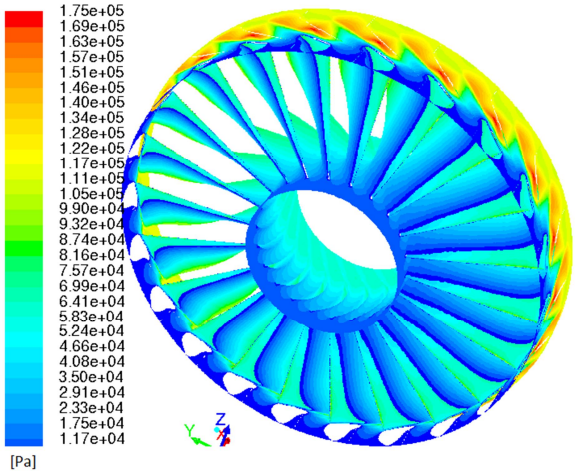

Figure 7. ROTOR 67 TOTAL PRESSURE CONTOURS AT DESIGN MASS FLOW RATE.

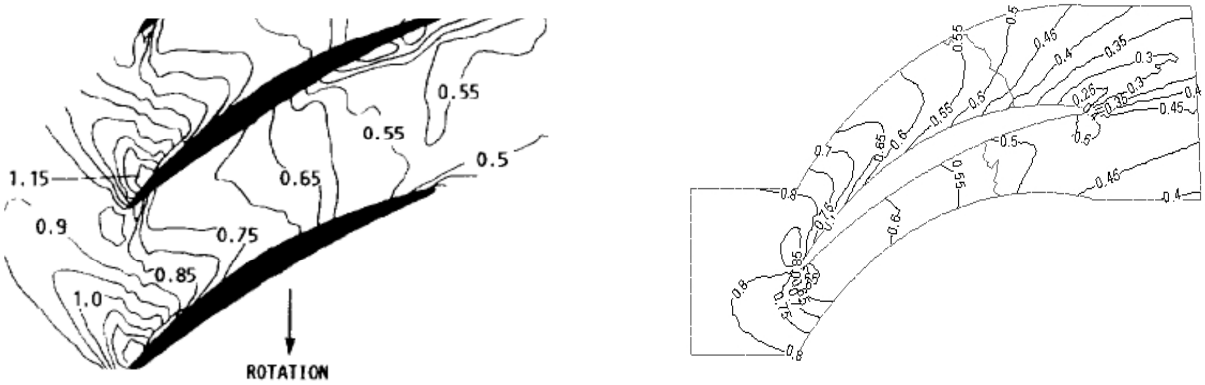

Figure 8. RELATIVE MACH NUMBER CONTOURS: EXPERIMENTAL [24] (LEFT) AND NUMERICAL (RIGHT) AT DESIGN MASS FLOW RATE.

numerical model calculates the overall flow structure correctly even if the relative Mach number is slightly underpredicted.
The trailing edge separation in the computation span is not discernible in the experiments.

Predicted flow with particles injection

In order to evaluate the erosion rate due to the ingestion of volcanic ash, a surface injection of solid particles was introduced in the modeling, assuming a mean particle velocity magnitude of 150 m/s, in accordance with the nominal speed at the fan inlet. Figure 9 shows the particle tracks around the rotor blades. The centrifugal force acting on particles drives particles toward the casing and thus avoiding the impact of particles with the part of the blade very close to the hub.
Erosion rate pattern, in terms of erosion rate (kg/m^2s), is shown in fig. 10. The erosion rate was used to evaluate the mass of blade material removed by impacting particles. The regions most exposed are a limited zone at the leading edge along almost the whole span and a zone at 30% of the span from hub, closer to the trailing edge. Near the leading edge blade pressure side is low exposed to particle flow so erosion effects are less visible in that zone.
The tip is not affected by particles impacts, so the tip clearance is constant, because of the centrifugal force acting on particles becomes more important as particle size increases, carrying particles toward the casing. Due to ash sample dimensions centrifugal effects are less significant .
Erosion rate values were used to modify the baseline geometry and to model the eroded geometry.

Predicted flow over eroded blades

For the modeling of the flow over the eroded geometry, the first step is the modification of the blade geometry on the basis of erosion damage. This can be done by using the predicted erosion rate patterns. So an equivalent erosion depth *lenght* was defined as:

$$L_{ER} = \frac{ER * \Delta t}{\rho} \quad (12)$$

Where ρ is the wall density and Δt the exposition time of the blades to particle impacts; we assumed a time of 1000 hours.
With an user-defined routine in C ++ the new nodes coordinates of the grid were obtained: for each node on the blades the equivalent erosion length and the normal to the node were calculated in order to compute the displacement value and orientation. The routine was implemented in the dynamic mesh module to obtain the modified grid corresponding to the predicted erosion rate pattern, assuming a one-step erosion change over 1000 hours.

In fig. 11 the eroded geometry, corresponding to the erosion pattern shown in fig. 10, is presented for the pressure side. It's evident the increase of surface roughness on respect to the baseline geometry, with a maximum wall distance, y+, at the wall boundaries close to 30.
The pressure side of the blade shows severe damage over wide region. The trailing edge is severely eroded rather than the leading edge. A particular of three different eroded blade sections is depicted in fig. 12 at different span distance from the hub.
This change in blade profile affects the flow field around the blade, as the relative Mach number, shown in fig. 13, and the static pressure (fig. 14). . The static pressure is no uniform and it is smaller than that of the uneroded blades, in particular near the trailing edge. It could be due to smaller boundary layer thickness due to the growth of surface roughness, and then the free stream velocity between the blades increases.
Table 2 describes in detail the percent degradation of the total pressure ratio due to particle ingestion in the fan for different mass flow rate; we can notice a mean reduction of about 10%, more significant for lower mass flow rate.

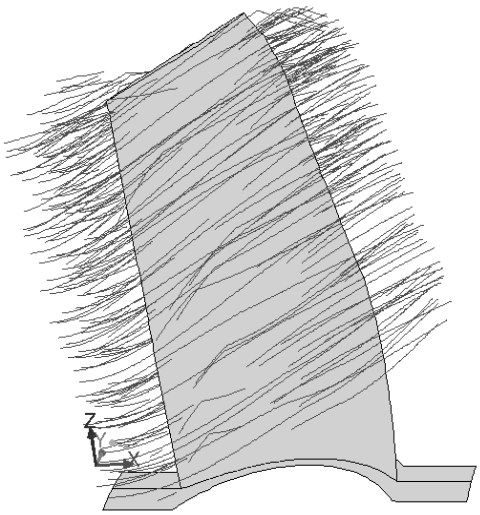

Figure 9. PARTICLE TRACKS AROUND THE BLADES.

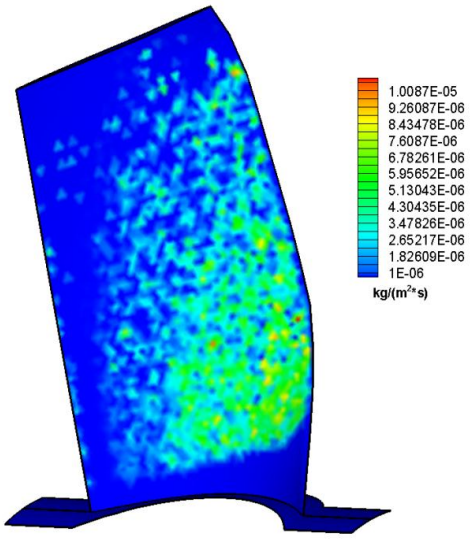

Figure 10: EROSION RATE PATTERN ON PRESSURE BLADE.

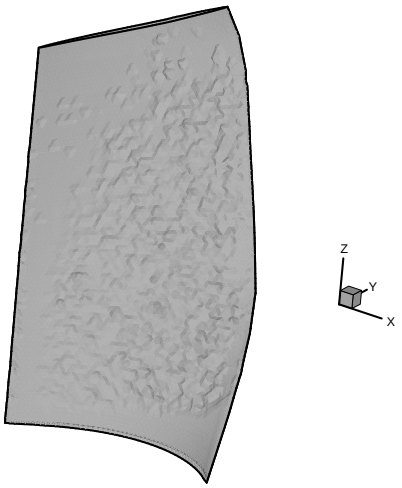

Figure 11. VIEW OF ERODED BLADE PRESSURE SIDE.

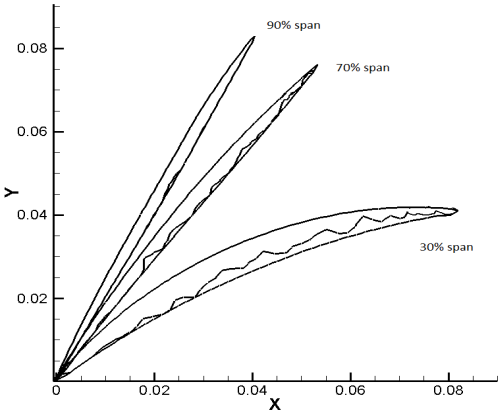

Figure 12. ERODED BLADE PROFILES AT 30%, 70% AND 90% SPANWISE FROM THE HUB.

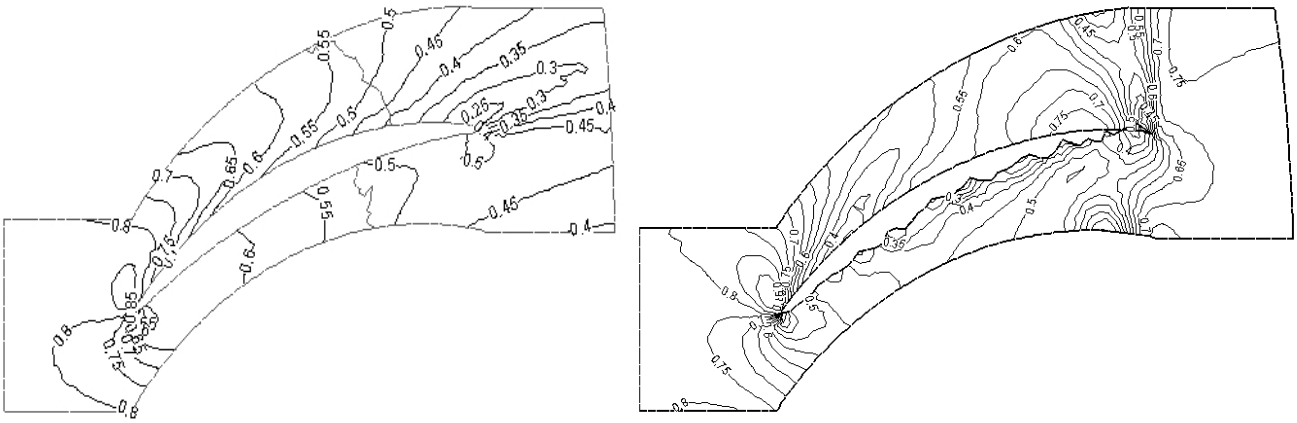

Figure 13. RELATIVE MACH NUMBER CONTOURS; BASELINE (LEFT) AND ERODED (RIGHT) CONFIGURATION.

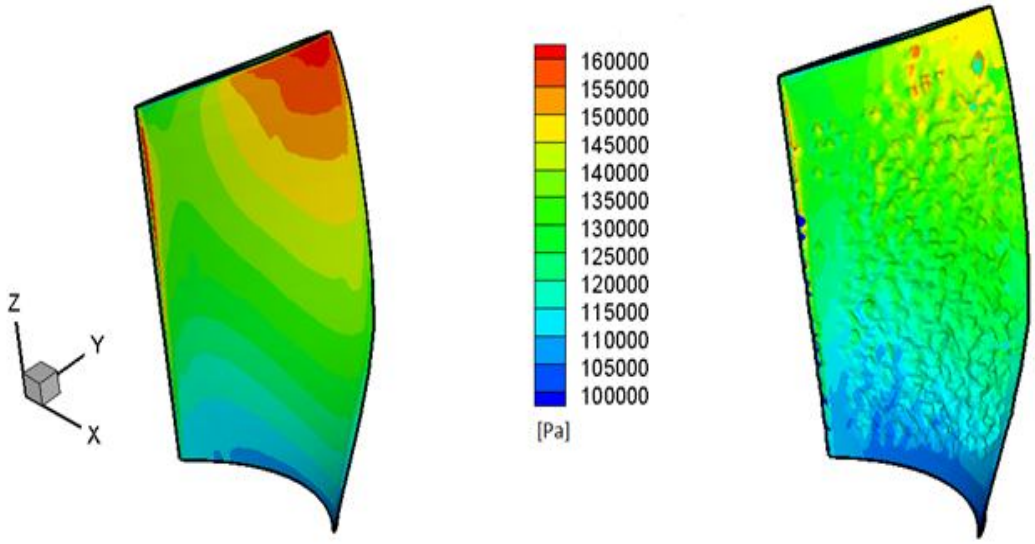

Figure 14. STATIC PRESSURE CONTOURS ON PRESSURE SIDE, BASELINE (LEFT) AND ERODED (RIGHT) GEOMETRY.

Table 2. PERFORMANCE DETERIORATION.

	Total Pressure ratio		
m/m_{ch}	Baseline geometry	Eroded geometry	Percent reduction [%]
0.92	1.6917	1.5087	**-10.82**
0.93	1.6885	1.5109	**-10.52**
0.94	1.6849	1.5127	**-10.22**
0.95	1.6825	1.5150	**-9.96**
0.96	1.6801	1.5160	**-9.77**
0.97	1.6623	1.5177	**-8.70**

CONCLUSIONS

NASA Rotor 67 has been investigated as test case for the prediction of performance degradation due to volcanic ash particle ingestion in aircraft engine. Several works studied erosion on turbomachinery blades, but few investigations were focused on the fluid dynamic on the eroded geometry. Besides for a reasonable prediction it is necessary to use quite realistic data about particles distributions and morphology. So in the present study a volcanic ash sample has been characterized by SEM analysis for morphological and dimensional analysis and the data has been used to model the particle ingestion.

The blade geometry has been modified with an user-defined routine based on the erosion rate patterns. Each node coordinate withstands a displacement proportional to the erosion depth in that node. The routine was implemented in the dynamic mesh module to obtain the modified grid corresponding to the predicted erosion rate pattern.

A comparison between the baseline geometry and eroded one is shown in order to quantify performance deterioration of the rotor. Obviously, being the fan the first component of an aircraft engine we can say that its performance deterioration spreads through the following components , resulting into a considerable reduction in aircraft engine overall efficiency. It was found that the reduction in terms of pressure ratio is 10% respect to pressure ratio in baseline configuration. Performance deterioration of the eroded fan diminishes with the increasing of its mass flow rate.

NOMENCLATURE

A	*surface area*
b_1, b_2, b_3, b_4	*Haider-Levenspiel equation coefficients*
d	*diameter*
$\bar{d}$	*mean diameter*
n	*rotational speed*
s	*particle path*
t	*time*
u	*longitudinal velocity*
$\bar{u}$	*longitudinal mean velocity*
u'	*instantaneous longitudinal velocity*
v	*lateral velocity*
w	*vertical velocity*
C	*particle diameter function*
C_D	*drag coefficient*
CFD	*Computational Fluid Dynamics*
ER	*erosion rate*
FD	*Fluent coefficient in particle motion equation*
L	*erosion equivalent length*
Re	*Reynolds number*
T	*time scale*
V	*particle velocity*
Y	*particles mass fraction*
α	*particle impact angle*
Φ	*sphericity*
μ	*fluid viscosity*
ρ	*density*

Subscripts and superscripts

ch	*choked condition*
ER	*erosion*
P	*volcanic ash particle*
sph	*sphere*
V	*volume*

ACKNOWLEDGMENTS

It is a pleasure to acknowledge L. Capodieci performed SEM measurements, L. Messina and M. D. Lo Castro for ash sample preparation.

REFERENCES

[1] Grindle, T. J., and Burcham, F. W. Jr., 2000, "Engine Damage to a NASA DC-8-72 Airplane From a High-Altitude Encounter With a Diffuse Volcanic Ash Cloud", NASA/TM-2003-212030.

[2] Miller, T.P., and Casadevall, T.J., 1999, "Volcanic Ash Hazards to Aviation," Encyclopedia of Volcanoes,page 915, 1999.

[3] Pieri, D. C., and Oeding R., 1991, "Preliminary Analyses of Volcanic Ash on an Aircraft Windscreen: the December 15, 1989 Redoubt Encounter," Airborne Hazards from Volcanic Ash Colloquium, Boeing Aircraft Company Seattle, Wash., USA.

[4] Hamed A., Singh D., and Tabakoff W., 1998, "Modeling of Compressor Performance Deterioration Due to Erosion", International Journal of Rotating Machinery, Vol. 4, No 4, pp. 243-248.

[5] Balan, C., and Tabakoff, W., 1983, "A Method of Predicting the Performance Deterioration of a Compressor Cascade Due to Sand Erosion", AIAA Paper No. 83-0178.

[6] Tabakoff, W., Lakshminarasimha, A.N., and Pasin, M., 1990, "Simulation of Compressor Performance Deterioration

Due to Erosion", ASME Journal of Turbomachinery, Vol. 112, No. 1, pp. 78-83.
[7] Muir, D.E., Saravanamutto, H.I.H., and Marshall, D.J., 1989, "Health Monitoring of Variable Geometry Turbines for the Canadian Navy", ASME Journal of Engineering for Gas Turbines and Power, Vol. 111, No. 2, pp. 244-250.
[8] Hamed A., and Tabakoff W., 2006, "Erosion and Deposition inTurbomachinery", Journal of Propulsion and Power, Vol. 22, No.2.
[9] Grant, G., and Tabakoff, W.,1975, "Erosion Prediction in Turbomachinery Resulting from Environmental Particles," Journal of Aircraft, Vol. 12, No. 5, 1975, pp. 471–478.
[10] Balan, C., and Tabakoff, W., 1984, "Axial Compressor Performance Deterioration" AIAA Paper 84-1208.
[11] Suzuki M., Inaba K. and Yamamoto M., 2007, "Numerical Simulation of Sand Erosion Phenomena in Rotor/Stator Interaction of Compressor", Proceedings of the 8th International Symposium on Experimental and Computational Aerothermodynamics of Internal Flows Lyon, ISAIF8-0093.
[12] Kumar A., Nair P. B. and Keane A. J., 2005, "Probabilistic Performance Analysis of Eroded Compressor Blades", Proceedings of Power ASME Power Conference, Chicago, IL, USA.
[13] Finnie, I., 1958,. "The mechanism of erosion of ductile metals", Proceedings of 3rd US National Congress of Applied Mechanics, pp. 527-532.
[14] Bitter, J. G. A., 1963, "A study of erosion phenomena part I", Wear, vol.6, pp.5-21.
[15] Bitter, J. G. A., 1963, "A study of erosion phenomena part II", Wear, vol.6, pp. 169-190.
[16] Neilson, J. H. and Gilchrist, A., 1968, "Erosion by a stream of solid particle", Wear, vol.11, pp. 111-122.
[17] Dobrowolski B. and Wydrych J., 2006, "Evaluation of Numerical Models for Prediction of Ares subjected to Erosion Wear", Int. J. of Applied Mechanics and Engineering, vol.11, No.4, pp. 735-749.
[18] Corsini A., Rispoli F., Sheard A.J., Venturini P., 2012, "Numerical Simulation of Coal Flt-Ash Erosion in an Induced Draft Fan", ASME Paper No. 2012-GT-9048, Copenhagen, Denmark.
[19] Ghenaiet A., 2012, "Effects of Solid Particle Ingestion through an HP Turbine", ASME Paper No. 2012-GT-69875, Copenhagen, Denmark.
[20] Hamed A., and Tabakoff, W., 1994, "Experimental and Numerical Simulations of the Effects of Ingested Particles in Gas Turbine Engines," Erosion, Corrosion and Foreign Object Effects in Gas Turbines, Von Karman Inst., Brussels.
[21] Mele D., Dellino P., Sulpizio R., and Braia G., 2011, "A systematic investigation on the aerodynamics of ash particles", Journal of Volcanology and Geothermal Research, Volume 203, pp. 1–11.
[22] Coltelli M., Miraglia L., and Scollo S., 2008 "Characterization of shape and terminal velocity of tephra particles erupted during the 2002 eruption of Etna volcano", Bull Volcano l 70:1103–1112, Italy.
[23] Ersoy O., 2012, "Surface area and volume measurements of volcanic ash particles by SEM stereoscopic imaging", Journal of Volcanology and Geothermal Research 190, pp. 290–296.
[24] Strazisar, A. J., Wood, J. R., Hathaway, M. D., and Suder, K. L., 1989, "Laser Anemometer Measurements in a Transonic Axial Flow Fan Rotor," NASA TP-2879.
[25] Narejo A.A., 2008, "3D Design and Simulations of NASA Rotor 67", Master's Thesys, University West, Trollhättan, Sweden.
[26] Iyengar V., 2004 "Advanced Control Techniques for Modern Compressor Rotors", School of Aerospace Engineering - Georgia Institute of Technology, Atlanta, GA;
[27] Ji L., Tian Y., Li W., Yi W., Wen Q., 2012, "Numerical Studies on Improving Performance of Rotor 67 by Blended Blade and Endwall Technique", ASME Paper No. 2012-GT-68535, Copenhagen, Denmark.
[28] Jinsheng W., Haiying Q., and Junzong Z., 2011, "Experimental study of settling and drag on cuboids with square base", Particuology 9, pp. 298–305.
[29] LabVIEW User Manual.
[30] ANSYS, Inc., 2009. "ANSYS FLUENT 12.0 Theory Guide".
[31] Fan, L., Yang, C., Yu, G. Z., and Mao, Z. S., 2003, "Empirical correlation of drag coefficient for settling slender particles with large aspect ratio", Journal of Chemical Industry and Engineering ,54, pp. 1501–1503, China.
[32] Gabitto, J., and Tsouris, C., 2008, "Drag coefficient and settling velocity for particles of cylindrical shape", Powder Technology, 183, pp. 314–322.
[33] Haider A., and Levenspiel O, 1989, "Drag coefficient and terminal velocity of spherical and non spherical particles", Powder Technol 58, pp.:63–70.
[34] Wydrych J., "Aerodynamic conditions of the erosion process in dust installations of power boilers", 2002, Ph.D. Thesis, 2002 Opole.
[35] Huser, A. & Kvernvold, O., 1998, "Prediction of sand erosion in process and pipe components", Proc. 1st North American Conference on Multiphase Technology, pp 217 – 227 Banff, Canada.
[36] Shih, T.-H., Liou, W. W., Shabbir, A. and Zhu, J., A, 1995. "New k-ε Eddy-Viscosity Model for High Reynolds Number Turbulent Flows - Model Development and Validation". Computers and Fluids, 24, pp. 227-238.
[37] Kim, S.-E., Choudhury, D., and Patel, B., 1997, "Computations of Complex Turbulent Flows Using the Commercial Code ANSYS FLUENT". Proceedings of the ICASE/LaRC/AFOSR Symposium on Modeling Complex Turbulent Flows, Hampton, Virginia.

